NATIONAL ENERGY TECHNOLOGY LABORATORY

OIL & GAS

DOE Award No.: FP00008137

Completed design information and description of measurements

(7/31/2019)

BEHAVIOR OF SEDIMENTS CONTAINING METHANE HYDRATE, WATER, AND GAS SUBJECTED TO GRADIENTS AND CHANGING CONDITIONS

Project Period (October 1, 2018 to September 30, 2019)

Submitted by:
Timothy J. Kneafsey

Signature

Lawrence Berkeley National Laboratory
DUNS # 078576738
1 Cyclotron Road
Berkeley CA 94720
Email: tjkneafsey@lbl.gov
Phone number: (510) 486-4414

Prepared for:
United States Department of Energy

July 31. 2019

National Energy Technology Laboratory

Office of Fossil

U.S. DEPARTMENT OF ENERGY | NATIONAL ENERGY TECHNOLOGY LABORATORY

DISCLAIMER

Completed design information and description of measurements

Timothy J. Kneafsey and Sharon E. Borglin

This report describes the completed test design information, measurements made, and their applicability to simulation. The tests have been designed to allow consolidation measurements on lab-made hydrate-bearing sediments. Two types of hydrate-bearing sediments are considered in the design – cementing and pore filling. The processes used, however, based on recent studies (*Lei et al.*, 2019), are likely to produce varieties of pore filling hydrate, with the cementing hydrate less likely to participate in the skeletal structure of the medium. Test and equipment design allows for both of these conditions.

Test and Equipment Design

Typical laboratory devices that are able to apply an effective stress on a methane hydrate-bearing sample use an elastomeric sleeve that contains the sample. Effective stress is applied hydrostatically (both radially and end to end) by a fluid outside of the sleeve. Any application of an effective stress close to zero risks leakage of fluids from inside the sleeve to the outside confining fluid, often carrying sand and eliminating the seal required for the experiment. One-dimensional consolidation is needed to model the test simulated by the Second International Gas Hydrate Code Comparison (IGHCC2), thus a rigid sleeve was selected, with a fixed platen at one side, and a floating (sliding) piston on the other (Figure 1). Both of these must seal tightly enough against the rigid sleeve, but the floating piston must be able to slide.

To make hydrate in the porous medium using the ice particle method, in which ice particles are mixed with freezing cold sand and that mixture is tamped into the sleeve, only very low effective stress can be used because compaction is not desired as the ice melts and hydrate is formed. This would reduce or eliminate the hydrate becoming part of the soil skeleton. The ability to provide no effective stress during hydrate formation is provided by pins that restrain the movement of the floating piston (Figure 1).

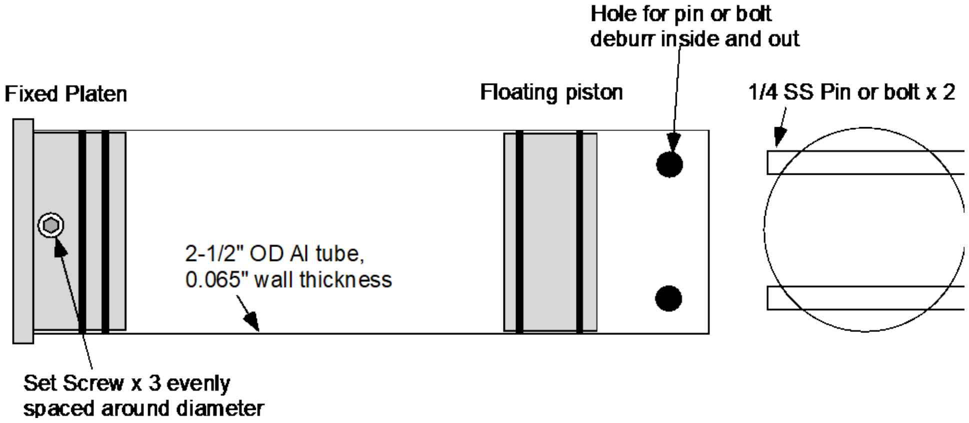

Figure 1. Detailed setup

Fixed platen and piston

The fixed platen has two o-rings and seals to the aluminum tube. A lip (shown on the left side in Figure 1) and three set screws hold it in place to the aluminum tube. A snowflake pattern is milled into the inside face of the platen. Initially, a circular groove was to be milled into the outside of the platen to contain a threaded aluminum tube (Figure 2). The purpose of the threaded aluminum tube was to allow more accurate location of the platen in space than the resolution of the CT scanner (0.625 mm slice thickness, also some slop on repeated scans). These were replaced with aluminum coupons set at angles to the axis of the platen, such that an axial displacement of the coupon would yield a lateral image shift governed by the angle of the coupon (Figure 3). The CT scanner has much better resolution in the lateral direction (0.193 mm), providing an improvement in locating the axial position of the platen. The coupons were potted into the plastic end piece with epoxy. Two small holes (~1/16 inch) were drilled blind from the outside that stop about 3/16 from the inside. A 1/16 inch diameter aluminum wire is potted into these holes to insure the orientation of the platen by X-ray CT.

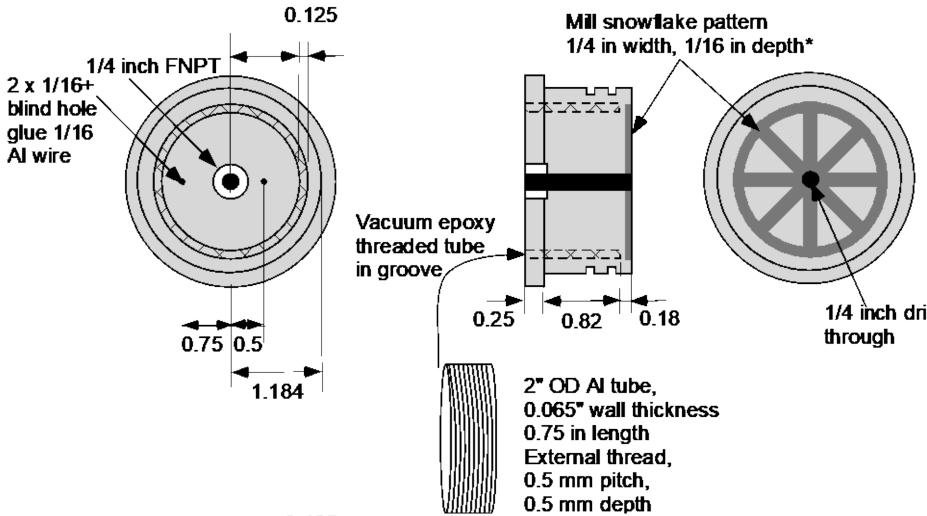

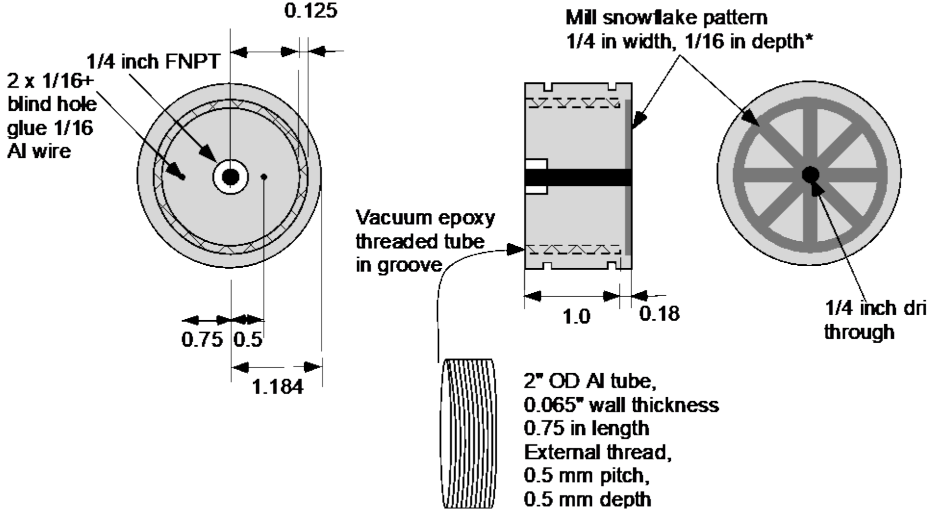

Figure 2. Initial end platen designs, top – fixed, bottom floating

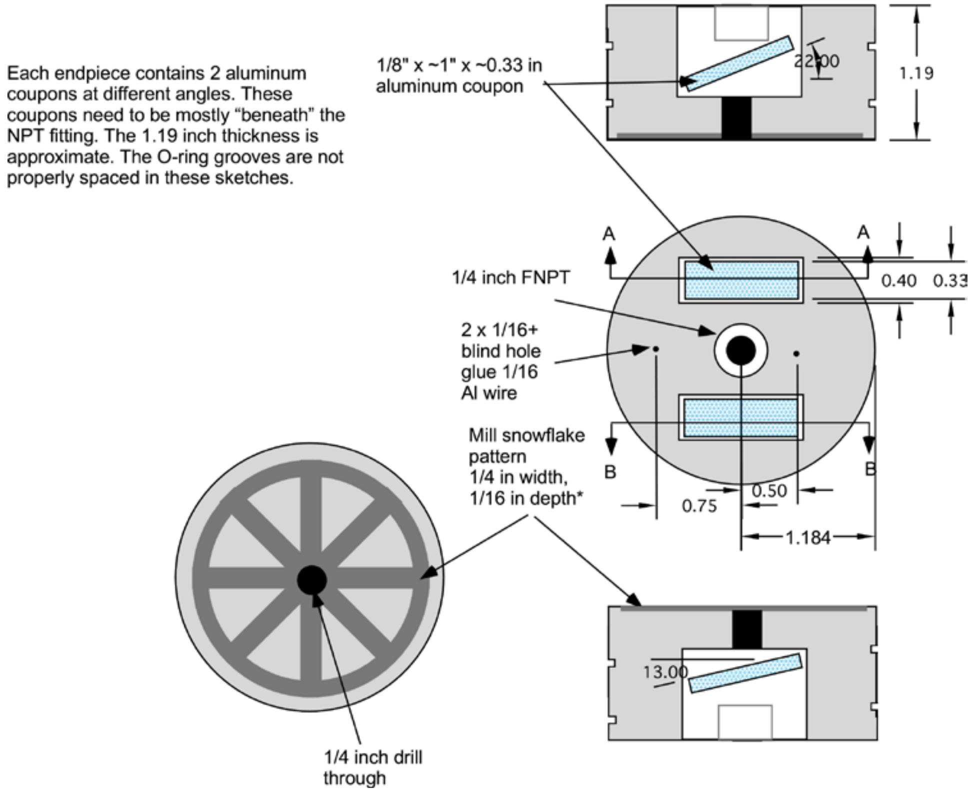

Figure 3. Current platen and piston design.

Measurements Made

For the cementing hydrate cases, the experiment procedure consists of mixing F110 silica sand and kaolinite (5% by mass) with water to the desired water content. The sand/clay mixture is packed into the rigid sleeve in small layers by tamping with flat-bottomed cylinders. The floating piston is inserted and pressed to the top of the sand by hand. The necessary plumbing and instrumentation (thermocouples) are attached to the piston, platen, and sleeve, and the assembly is placed in the pressure vessel and filled with confining fluid (propylene glycol antifreeze and water) (Figure 4). The pore pressure is increased with methane in increments as the external confining pressure is increased such that the sample experiences a maximum of 100 psi confinement. When the desired pressure is attained, the temperature is lowered to allow hydrate to form. The quantity of gas added and the initial quantity of water are knowns, aiding in computing the amount of hydrate conversion. Once hydrate has formed, the sample is saturated with water by introducing fresh water slowly into the sample. After sample saturation, the effective stress is adjusted to the desired level by maintaining the pore pressure at a constant desired value and adjusting the confining pressure within the rating of the pressure vessel.

Figure 4. left - assembled sleeve with sample on vessel endpiece. Right – floating piston with pins to restrict motion away from the sample.

Two methods can be used to assess the sample compaction: CT scanning and confining fluid volume changes. Both methods have their advantages and disadvantages. The CT scanner is not well suited to monitor frequent temporal changes in piston displacement, because of cost of operation. Resolution is another issue, however, sub-slice thickness resolution is now being achieved (see below). Confining fluid volume can be read and recorded directly from the confining pump. If there are no leaks, or if the leaks can be corrected, the temporal behavior can be quantified.

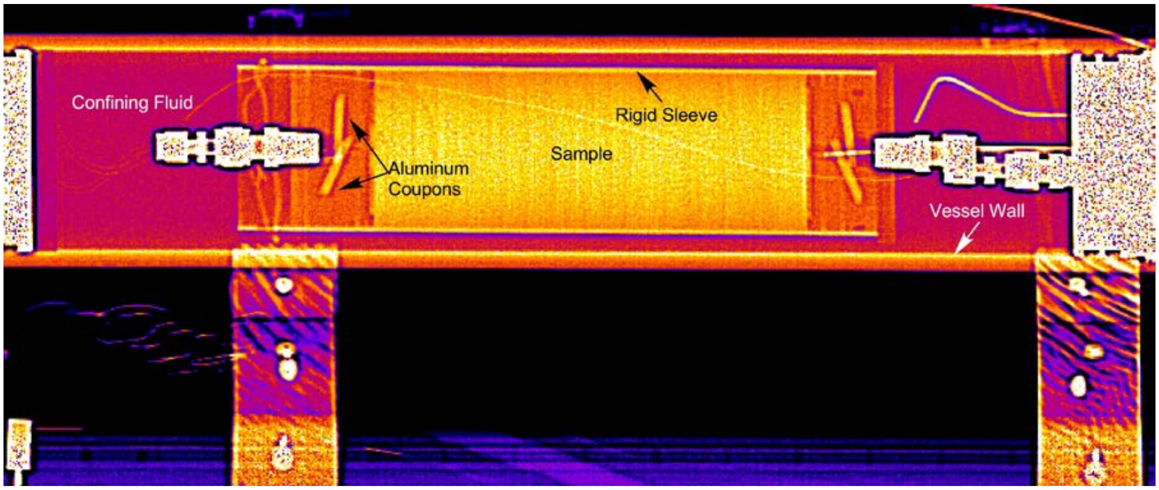

Figure 5. X-ray image of assembled system. The sample is in the center (yellow) with the fixed platen to the right and the floating piston to the left. The aluminum coupons are visible within the platen and piston. All of this is contained in the rigid sleeve, inside the pressure vessel.

An example of measurements made is presented below. Sand containing 5% kaolinite by mass was moistened to provide 30% water saturation. The mix was packed into the sleeve that was attached to the fixed platen. When the proper amount was added and tamped down, the floating piston was inserted and the assembly was plumbed and instrumented as stated above. As usual, temperature at numerous locations and pressure (system, pressure indicated by pumps) were recorded over time. CT scans were taken at appropriate junctures (initial, hydrate-bearing, water saturated, and at each effective stress endpoint).

The use of a medical CT scanner to make high resolution displacement measurements has been problematic in the past, even to account for nonrepeatability (slop) in table movement. Using the new platen and piston, scans were taken including the aluminum coupons. Earlier tests taught us that registration (alignment) in the x-y directions of two sets of data had to be as precise as possible, and good in the z (axial) direction. The best registration in the z direction occurs when the CT scanner is kept in operating mode. The instrument limits this time duration, but if it is manipulated frequently enough, it will remain in operating mode. That keeps the table elevation the same, and the table locked on the actuator. A re-setup requires changing the table elevation, and because the elevation is controlled by rotating lever arms, the table elevation affects the z location. The analysis methods derived here may improve this problem.

Many registration algorithms align slices using a center-of-mass approach. Since our center of mass changes with process, this can make the process difficult. We use an existing registration algorithm (Image Stabilizer Li, 2008), but eliminate the center of mass problem by copying our stack of images, selecting the portion of interest in one copy, setting that region to a single distinct value, and aligning the stack to a reference image. Image Stabilizer provides a record of image translations used to align the stack. We then apply that record to the other copy. Since we use the same reference standard for all stacks, the stacks are well registered. This is verified by subtracting one stack of registered images from another and examining them. Subtraction of poorly registered images will show bright features on one side, and dark on the other (Figure 6 left), whereas a subtraction of properly registered images will not (Figure 6 right). An ImageJ (*Rasband*, 2016) macro describing the process is included in the appendix.

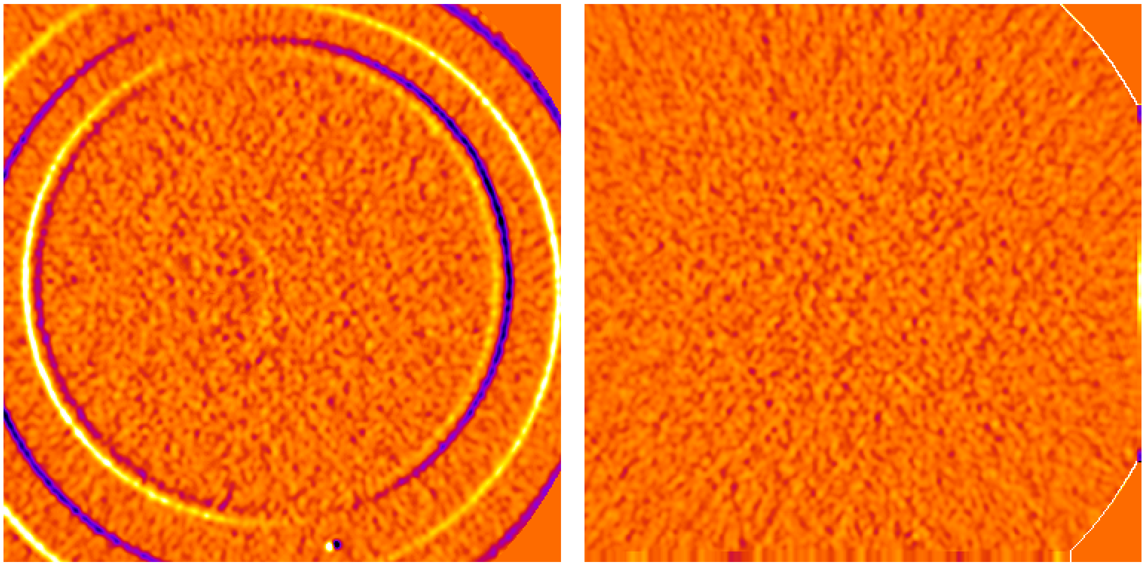

Figure 6. Subtracted unregistered (left) and registered stacks (same location). Note image on right has been cropped but includes the center circle shown on the left. The artifacts in the right corners of the registered stacks shows regions where there were no data in the images.

Once registered, a single slice was selected from each data set that intersected the aluminum coupon on each side of the sample. A profile crossing the aluminum coupon in the CT data was extracted from each set of scans, and the translation of the feature, considering the geometry of the coupon, was used to compute the axial translation of the platen or piston (Figure 7). From those 2 translations, the compaction of the sample can be computed. An example of the compaction data is shown in Figure 8. Note that the slice thickness is 0.625 mm, and nearly all the measurements are smaller than that.

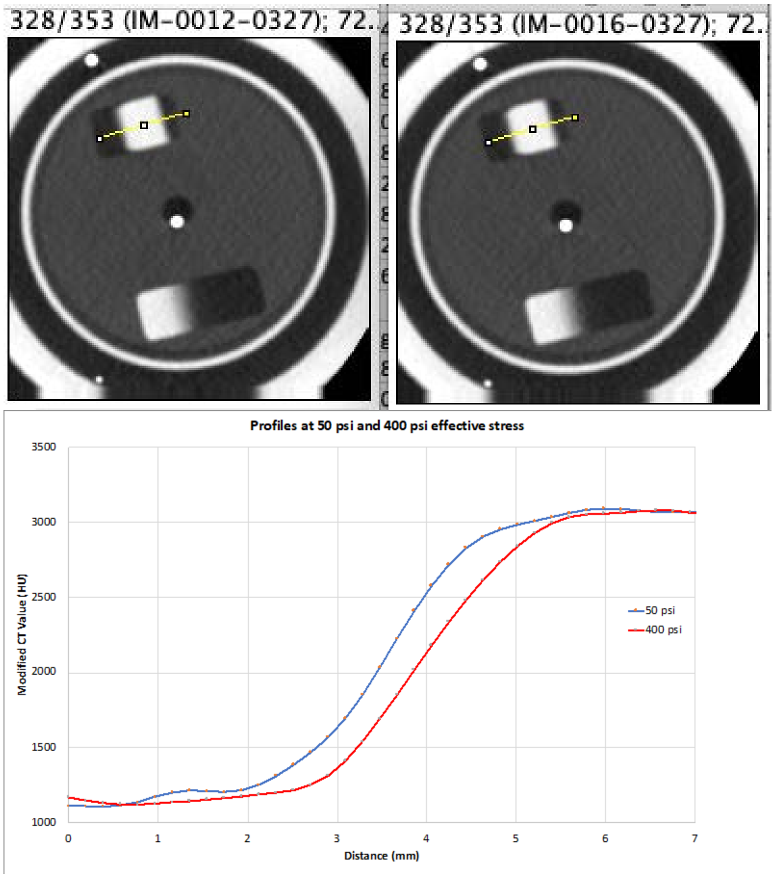

Figure 7. Corresponding slices at 50 psi effective stress (top left), and 400 psi effective stress (top right). Modified CT values for the highlighted profile line, placed in the exact same location in each frame.

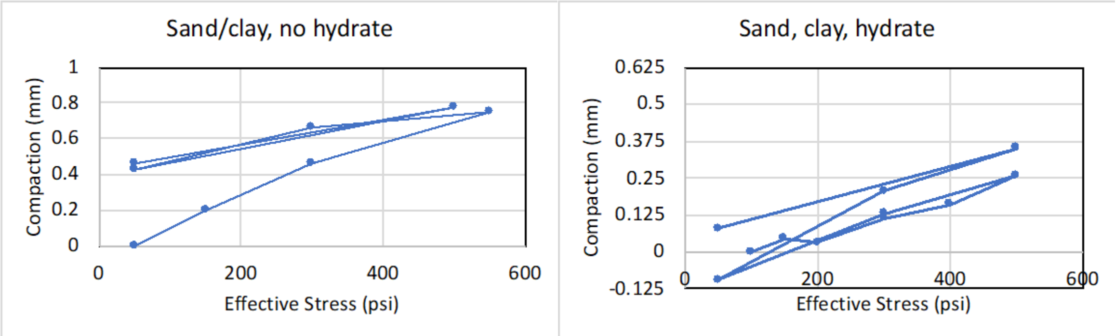

Figure 8. Compaction of a sand/clay sample (left) and a sand/clay/hydrate sample (right).

Observations

Briefly, two observations are mentioned here.

1. During the sample saturation, clay was observed to migrate. This is in contrast to many of our previous studies, but in agreement with studies performed by many others.

2. The impact of the snowflake pattern milled into the piston for fluid distribution was observed several slices into the sample. In response to this, the pattern will be filled in.

Applicability to simulation

The data collected here are suitable to be compared to simulations. Several points need to be considered.

1. Hydrate formation is rarely uniform, although Kneafsey et al (2010) (*Kneafsey et al.*, 2010) showed fairly uniform hydrate formation in similar sand/clay samples. This will make interpretation of the measurements interesting and provide different viewpoints.
2. Samples used here are long compared to typical samples. This length was selected to maximize the compaction length. Compaction may occur over only a limited portion of the sample however. A strain of 10^{-3} in a 25 mm thick sample might either be 6 x 10^{-3} in a 150 mm sample if acting over the entire sample, or interpreted as 1.6 x 10^{-4} if action only over that 25 mm. Current data sets will be strongly considered prior to continuing.

Conclusions

A consolidometer was constructed that allows the measurement of strain on hydrate-bearing samples. The strain is computed from X-ray CT scans, using a custom platen and piston containing aluminum coupons at angles to the axis of the scanning. These allow computation of sub-layer thickness displacements. Precise image registration is required to employ this strategy. To allow for this, a new very successful technique was devised and employed. Adding to the success was the refined usage of the CT scanner itself. Two other techniques are under consideration to improve and make the displacement measurements automatic.

References

Kneafsey, T.J., Y. Seol, A. Gupta, and L. Tomutsa (2010), Permeability of Laboratory-Formed Methane-Hydrate-Bearing Sand: Measurements and Observations Using X-Ray Computed Tomography, *SPE Journal*, doi:10.2118/139525-pa.

Lei, L., Y. Seol, J.-H. Choi, and T.J. Kneafsey (2019), Pore habit of methane hydrate and its evolution in sediment matrix – Laboratory visualization with phase-contrast micro-CT, *Marine and Petroleum Geology*, *104*, 451-467, doi:https://doi.org/10.1016/j.marpetgeo.2019.04.004.

Li, K "The image stabilizer plugin for ImageJ," http://www.cs.cmu.edu/~kangli/code/Image_Stabilizer.html, February, 2008).

Rasband, W.S. (2016), ImageJ, edited, U. S. National Institutes of Health, Bethesda, Maryland, USA, doi: http://imagej.nih.gov/ij/.

Appendix – Image Registration Technique implemented in ImageJ.

```
//to modify for new file, check file name in line 2 and line 37.  Also check number of
slices in line 40.  A 'Reg_standard.tif' file needs to be open.    Rectangle line 6 and
threshold line 11 may need adjustment.
//changename
selectWindow("XXXX");
run("Duplicate...", "duplicate");
rename("stack-1");
selectWindow("stack-1");
setSlice(1);
run("Add Slice");
setSlice(1);
selectWindow("Reg_Standard.tif");
run("Select All");
run("Copy");
selectWindow("stack-1");
setSlice(1);
run("Paste");
setSlice(1);
makeRectangle(108, 62, 375, 375);
run("Crop");
run("Add...", "value=1024 stack");
setAutoThreshold("Default");
//run("Threshold...");
setThreshold(1324, 5168);
run("Analyze Particles...", "size=10-Infinity show=Masks exclude include stack");

run("Image Stabilizer", "transformation=Translation maximum_pyramid_levels=1
template_update_coefficient=1 maximum_iterations=200 error_tolerance=0.0000001
log_transformation_coefficients output_to_a_new_stack");
selectWindow("stack-1");
run("Image Stabilizer Log Applier", "output_to_a_new_stack");
//changename
rename("XXXX");
//changename
```

```
saveAs("Tiff", "/Users/XXXX/Documents/Projects/Hydrate/NETL Hydrate/FY19/TerzaghiProblemExpData/XXXX.tif");
setSlice(1);
run("Delete Slice");
run("Properties...", "channels=1 slices=352 frames=1 unit=pixel pixel_width=0.195 pixel_height=0.195 voxel_depth=0.625");
run("Fire");
run("Enhance Contrast", "saturated=0.35");
selectWindow("stack-1");
run("Close");
selectWindow("Stablized Mask");
run("Close");
selectWindow("Mask of stack-1");
run("Close");
selectWindow("Mask.log");
run("Close");
```

National Energy Technology Laboratory

626 Cochrans Mill Road
P.O. Box 10940
Pittsburgh, PA 15236-0940

3610 Collins Ferry Road
P.O. Box 880
Morgantown, WV 26507-0880

1450 Queen Avenue SW
Albany, OR 97321-2198

Arctic Energy Office
420 L Street, Suite 305
Anchorage, AK 99501

Visit the NETL website at:
www.netl.doe.gov

Customer Service Line:
1-800-553-7681

NETL NATIONAL ENERGY TECHNOLOGY LABORATORY

U.S. DEPARTMENT OF ENERGY | NATIONAL ENERGY TECHNOLOGY LABORATORY